Vertically Stratified Flows in Microchannels. Computational Simulations and Applications to Solvent Extraction and Ion Exchange

ARTICLE *in* ANALYTICAL CHEMISTRY · JULY 2003

Impact Factor: 5.64 · DOI: 10.1021/ac0340713 · Source: PubMed

3 AUTHORS, INCLUDING:

Petr Kubáň
Tallinn University of Technology
69 PUBLICATIONS **1,575** CITATIONS
SEE PROFILE

Jordan M Berg
Texas Tech University
130 PUBLICATIONS **1,437** CITATIONS
SEE PROFILE

Vertically Stratified Flows in Microchannels. Computational Simulations and Applications to Solvent Extraction and Ion Exchange.

Petr Kuban[1†], Jordan Berg[2] and Purnedu K. Dasgupta[1]

[1]*Department of Chemistry and Biochemistry*
[2]*Department of Mechanical Engineering*
Texas Tech University, Lubbock, TX, 79409, USA.

ABSTRACT

In this paper we describe the conditions under which two immiscible fluids flow atop one another (viewed perpendicular to the plane on which the channel is inscribed) in a shallow microfluidic channel. First, we predict the behavior of a two-phase system using fluid dynamic simulations with water-butanol and water-chloroform as model systems. We numerically model effect of various physical parameters, such as interfacial surface tension, density, viscosity, wall contact angle and flow velocity on the type of flow observed and find that interfacial surface tension and viscosity are the parameters responsible for formation of vertically stratified, side-by-side or segmented flows. As predicted by numerical simulations, water-chloroform system never assumes a vertically stratified configuration, while water-butanol system does when the two liquids flow at sufficiently high flow velocities. In actual experiments, we test conditions under which potentially useful two-phase systems form stable vertically stratified flows. We also demonstrate that compared to side-by-side flow schemes, shorter diffusion paths are achievable and thus the system can be used at higher flow rates to obtain the same performance. We then apply such findings to practical analytical problems such as solvent extraction and ion exchange.

---

* corresponding author
Email address: Sandy.dasgupta@ttu.edu

† Permanent Address: Department of Chemistry and Biochemistry, Mendel University, Zemedelska 1, CZ-61300, Brno, Czech Republic

Introduction

In a previous paper, we described a microscale continuous ion exchanger in which ion exchange takes place at the interface between two immiscible liquids.[1] In that work, as in the work of many others, [2-14] as well as the commercially available H-filter or T-sensor devices,[15] two or more liquid streams flow side-by-side. This description has the implicit understanding that the relevant microfabricated devices have a planar format where relatively long but shallow channels are inscribed on the plane with the largest surface area. The liquid streams flow side-by-side when viewed in a direction perpendicular to the large plane. In the present work, we are interested in flow of liquid streams that are vertically stratified, i.e., when viewed from a direction perpendicular to the largest plane, the liquids flow atop each other. It needs to be made clear at the outset that in referring to vertical stratification, it is not the influence of gravity that we are concerned with. In other words, if a conventionally operated device with side-by-side liquid flows is turned on its side, in reference to gravitational forces the liquids do flow atop each other. This is *not* the situation we refer to. In a typical microfabricated channel, the channel width w is equal to or greater than the channel depth d. We are interested in situations where the interface between the liquids is defined by the channel length l and the width w. As such, we are interested in situations where an increase in the channel width w will result in a direct and concomitant increase in the liquid interfacial area and thus also an increase in the overall mass transfer rate. The performance of such a flow geometry is obviously scalable with the channel width whereas an increase in the channel width in side-by-side flow geometries results in no significant gain.

Recently efforts have been made where two immiscible liquid streams do flow atop each other.[16] However in such experiments, the device consists of two partially overlapping channels with the overlap being at maximum about 20% of the channel width as a compromise between the flow stability and mass transfer enhancement. Others have selectively altered the surface characteristics of portions of a flow channel to achieve surface-directed flow[17,18]. In one recent example, separate and geometrically non-coincident flow channels were inscribed on a top and a bottom glass plate and one of the plates was modified with octadecylsilane to render it hydrophobic. Nitrobenzene and water flowed in 250 μm wide channels and interacted only in a small region where the two channels passed across each other.[19] The maximum pressure difference that can maintain stably segregated liquid flows based on surface-direction is not large; pressure and channel curvature limits have been discussed.[17,18]

It should be obvious from the above that simply introducing two fluids atop one another in a flow channel does not necessarily result in stable stratified flow. In fact, under most conditions, this results in rapid conversion to dispersed or segmented flow of the phases downstream. In this work, we explore first by computational fluid dynamic simulations the conditions that impart stability to vertically stratified flows (without any selective surface modification) and then apply this to practical analytical problems involving solvent extraction and ion exchange.

Simulation Studies

Interfacial stability in two flowing fluids has been much studied. Mismatched velocities at the interface tend to produce vortices, often referred to as Kelvin-Helmholtz instability

(KHI), see [20] for a graphic simulation. Two fluids of differing densities in a gravitational field (or under acceleration) may exhibit Taylor or Rayleigh-Taylor (RT) instabilities, for a graphic example of two fluids differing in density by a factor of 2 and exhibiting RT/KHI instability, see [21]. For an analytical treatment of these and other interesting cases, see [22]. Two-phase flows of water and steam have been especially studied due to their importance in practical applications. Even in this one-component two-phase system, it is well known that velocity, surface tension, viscosity and density effects are all important and flow can occur in a variety of regimes including bubbly, stratified, wavy, plug, slug, annular and dispersed [23]. In the following, we carry out parametric variations (relevant to experiments described later) in a numerical computation domain to determine when stable stratified flow occurs or breaks down. Binary fluid flows were chosen from chloroform, water and butanol because these fluids represent a large range of relevant physical properties over which behavior could be examined.

The simulated flow took place in a 2 x 45 x 0.4 mm (x·y·z, width-length-depth) channel. Liquids enter the channel at $y = 0$ with specified, equal velocity with one fluid occupying the upper ($0 < z < 200$ μm) and the other occupying the lower half (-200 μm $< z < 0$). The fluids exit at ambient pressure at the $y = 45$ mm plane. To reduce the computation time, a centerline symmetry condition is applied. This means that the simulation enforces a reflective symmetry about the plane $x = 0$; e.g the flow in only the right-half side of the channel is modeled. This reduces computation time at least by a factor of 2. However, some possible flow configurations, such as a two stream side-by-side flow do not exhibit this symmetry, therefore cannot be captured in this particular

simulation. The unconstrained case will be addressed in future work. Results for two flow situations are presented here: (a) butanol enters atop water, (b) water enters atop chloroform. Gravity is attractive in the negative *z* direction and thus density effects favor stable vertical stratification in both cases. Initially, the channel is entirely filled with the primary fluid, water. The simulation is run at least until the secondary fluid reaches the outlet.

Figure 1 shows the results as a function of the input velocities. Over the range studied, the water/chloroform flow always segments while for butanol/water there is a clear transition from a segmented flow (flow velocities less than 10 mm/s) to a side-by side three layer flow with water in the center (flow velocities between 10 mm/s and 20 mm/s) and stratified flow. Stratified flow is the stable configuration at higher flow rates. Note that due to the symmetry enforced by the simulation boundary conditions, the present simulation cannot really distinguish two-phase side-by-side flow from three phase side by side flow. The most computationally intensive aspect of the simulation is tracking of a moving interface. While in stratified flow the interface is essentially stationary, in segmented flow multiple interfaces move at the bulk fluid velocity. The simulated butanol/water stratified flow was observed to become stable at inlet flow rates above a critical value somewhere between 15 and 20 mm s^{-1}. The side-by-side configuration appears to play the role of a transition regime. Indeed all three configurations (segmented, side by side and vertically stratified) were observed experimentally; video clips (~5 MB) will be sent to readers on request. It is interesting that these results are not intuitive. It would be normal to expect that the large density difference in the water/chloroform case would more easily lead to stable stratified flow

than for butanol/water. In one-component two-phase flow, a transition is observed from stratified to "plug" flow (akin to segmented flow) as flow rate increases [22]. Accordingly, in the butanol/water case, it may seem logical to anticipate that high flow velocities will disrupt a stable stratification, rather than aid it. The reverse is predicted from the simulations. Experiments bear out these counterintuitive numerical predictions. The obvious logical question remains as to what physical factors are the most responsible for achieving stable stratified flow. Since the above isothermal simulations capture the essential behavior observed experimentally (see below), the role of thermal gradient effects such as buoyancy and surface tension driven convection need not be considered. No dissolved solutes and no activity gradients in solutes were incorporated in the model, so chemical effects can also be deferred. Turning gravitational forces off computationally does not significantly change the flow patterns (reversing gravitational orientation experimentally similarly has little or no effect, *vide infra*), hence we may also eliminate these from immediate consideration. We carried out numerical experiments with a constant inlet velocity of 20 mm s^{-1} (since this leads to stratified flow in butanol/water and segmented flow in water/chloroform cases, either experimentally or numerically) under a variety of hypothetical situations. A single-fluid simulation using water results in parallel streamlines for the entire channel length, i. e., stable stratified flow results. This in itself is of interest because for water based fluids such as blood and isotonic saline will be expected to behave similarly and it should be possible to scale up the membraneless dialyzers such as the H-filter. (An obvious but ambitious extension will be a multitiered microfabricated hemodialyzer).

Proceeding in this hypothetical scenario where two fluids, both having the density and viscosity of water and no interfacial tension between them flow in a stable stratified manner, we changed the density and viscosity of the bottom fluid to those for chloroform but the interfacial tension was still left at zero. Numerical predictions suggested that stable stratified flow was maintained. Then we altered the density and the viscosity of the bottom fluid back to that for water but this time set the interfacial tension between the two fluids to that for chloroform-water. The boundary contact angle values were set to experimentally observed chloroform-water-glass values as well. Numerical predictions indicated that flow would become segmented, leading to the conclusion that in this case interfacial tension is a more important contributor to flow morphology than density and viscosity.

To explore this further, the interfacial tension parameters were replaced by those of the butanol/water system. While we expected stratified flow based on the earlier butanol/water simulations, segmented flow was numerically predicted. Allowing the top inlet fluid to have the density of butanol and turning on gravity did not change this situation. Only after the viscosity of the top fluid was also increased to the value for butanol, stratified flow became stable. In this case, the high viscosity of butanol is necessary to stabilize stratified flow even though the interfacial tension of butanol-water is small. We also performed a preliminary study of the role of the wall contact angle in the butanol/water system. The results indicated that a contact angle of near 90 degrees is preferred for stratified flow, and that departures greater than 10 degrees in either direction can cause the flow to segment.

In this section, we primarily intend to establish the applicability of computational fluid dynamics (numerical modeling) to examine stratified flow. More, and more detailed work is necessary for better understanding and complete characterization. Extremes of values, e.g., putting in parameters of mercury and water, cause intrinsic instability in the numerical system. Nevertheless, as discussed in the experimental results, the present numerical simulations are at least qualitatively verified by the experiments.

EXPERIMENTAL

Numerical Simulations

Numerical simulations were carried out with the using the Free Surface module of CFD-ACE software package[24] to model the fluid-fluid interface. Two fluids (designated primary and secondary) are assumed to be completely immiscible, and their velocities are assumed to be equal at the interface (no KHI). The algorithm relies on a volume-of-fluid (VOF) interface tracking scheme[25], which propagates a scalar variable, F, describing the fill fraction of the secondary fluid that evolves according to $\frac{\partial F}{\partial t} + \nabla \cdot vF = 0$ where v is the velocity vector. The algorithm uses a piecewise linear interface construction method[23] to incorporate surface tension forces. The VOF module also allows surface tension effects normal and tangential to the interface. The normal force due to surface tension is assumed proportional to the mean curvature of the interface, while the tangential force, if included, typically arises due to temperature or species concentration gradients along the interface. The existence of both normal and tangential forces were allowed in our simulations, although under the isothermal conditions and without any gradient in dissolved species there should be little or no tangential force. The explicit solver option was used. The overall computational time depends of course on the choice of the time step, increasing with a decreasing time step. However, interface-tracking problems can become numerically unstable if the time step is too large, and the Courant-Friedrich-Lewy (CFL) condition is violated.[26] We allowed the VOF module to automatically adjust

the time step based on the interface velocity.[23] The simulation times were, however, quite large, typically requiring 6-72 hours on a Pentium IV class processor running at 1.4 GHz with access to 512 MB RAM; this is perhaps at the practical limits of PC-based computations.

Fluid-wall interface effects are handled by specifying for each solid boundary the interface contact angle at fluid-fluid-wall triple points. These values were estimated by examining the glass-chloroform-water and glass-butanol-water triple points in square glass cuvettes. In the glass-chloroform-water system we specify the angle at the triple point between the chloroform-glass interface and the chloroform-water interface. In the glass-butanol-water system we specify the angle at the triple point between the butanol-glass interface and the butanol-water interface. The actual experiment contains several different wetted materials as part of the fluid channel, including glass, polyester (printer transparency film), polyvinyl chloride (electrical tape). Thus, there may be fairly large uncertainty in these values. The following values were provided as input to the VOF module: Interfacial tensions: Water-butanol and water-chloroform 2.1 and 32.8 mN/m, respectively;[27] contact angles: water-butanol-glass and water-chloroform-glass 97° and 74°, respectively.

The continuity and momentum equations that govern the fluid velocity and the pressures are solved using the flow module.[23] The density and dynamic viscosity inputs provided to the flow module come from standard compilations and respectively were: water (1003 kg/m^3, 0.855 g/m·s), butanol (798 kg/m^3, 2.5 g/m·s) and chloroform (1480 kg/m^3, 0.540 g/m·s). Velocity boundary conditions are applied at the inlet and varied from run to run as described. Atmospheric pressure was specified at the outlet boundary surface. No-slip conditions were applied along the channel walls.

Initial work showed that both the stratified and segmented flow patterns observed during the simulations exhibit mirror-image symmetry on both sides of the x-axis. This symmetry was exploited to reduce the total mesh size and reduce computing time by limiting the computations to only the positive side of the x-axis ($0<x<1$ mm).
The resulting geometry was meshed uniformly using hexahedral ("brick") elements. Seven elements were used to mesh the x-dimension, eight elements were used to mesh

the *z*-dimension, and 179 elements were used to mesh the *y*-dimension. Thus the total number of elements was 10,024.

Device. The device, shown schematically in Figure 2, was constructed from two glass slides GS1 and GS2 (25 x 75 x 1 mm) separated by 150-400 μm with three layers of spacers. At *x,y* coordinates of 15,12 and 60, 12 mm, a hole (0.75 mm dia) each was drilled into GS1 and GS 2 defining access to a 45-mm long straight flow path. The four inlet/outlet stainless steel tubes (not shown, 575 μm i.d., 1.05 mm o.d.) were cemented to the holes with epoxy adhesive. The flow channel between the two glass slides was formed by a three-layer spacer. Either black electric tape (3M, thickness 150 μm) or Kapton polyimide tape (Fralok, Canoga Park, CA, thickness 80 or 50 μm) was used as the outer gaskets G1 and G2 and defined the boundaries of the flow channel. The intermediate gasket T was made from a polyester transparency sheet (thickness 50 or 80 μm, an 8 mm portion of this stuck out like a tongue into the flow channel on the entrance side. Depending on the specific spacer elements chosen, the channel depth could be varied from 150-380 μm, with the internal volume correspondingly varying from 10 to 30 μL.

Because the hydraulic resistance of the device was small and even a 10 cm hydrostatic head produced flow rates much higher than that desired, liquid flows were achieved by aspiration with a peristaltic pump (Dynamax, Rainin) from the device outlets at 20-160 μL/min. The liquids were aspirated at given flow rates from both outlets, thus the total volumetric flow rate was the sum of the individual flow rates from the outlets. The inlet liquid reservoirs were connected to the device with large bore (1.25 mm i.d.) tubes to eliminate any flow resistance. Nominally the inlet reservoirs were maintained at a hydrostatic height of 20 cm. However, the reservoir heights could be adjusted relative to each other to change the head pressure and thus modify the thickness of the fluid layers flowing through the device. (Note that while recent surface-directed flow experiments

could operate only over pressure limits of +300 to –200 Pa, a head pressure of 20 cm H_2O is equal to ~2000 Pa). We made no attempts to find the maximum pressure limit for stable stratified flow.

Injection/Detection. A six-port rotary injector (Rheodyne) with a 5-μL loop volume was used for sample injection. Absorbance measurements were made with an on-capillary detector (model CV^4, ISCO, Lincoln, NE). A fused silica capillary (o.d. 353 μm, i.d. 180 μm) was connected directly to the microfluidic device outlet by inserting it inside the outlet tube and thus to minimize the dispersion. The absorbance of the organic phase was measured at 656 nm (extraction of methylene blue) or 372 nm (extraction of chromate).

For off-line absorbance measurement experiments, effluent from the device were collected, diluted if necessary, and measured on a HP 8453 spectrophotometer. The conductivity detection electrodes were constituted of a concentric cell consisting of an inner stainless steel tube (175 μm id, 350 μm od) and an outer stainless tube (575 μm id, 1.05 mm od) separated by a PTFE tube acting as a spacer. This assembly was placed in the exit of the channel used for the aqueous eluent phase. The electrodes were connected to an early model commercial conductivity detector (Model CDM-1, Dionex Corp.). No preamplifier was used and S/N was not optimized

Chemicals. All chemicals were of reagent grade. Aqueous stock solutions of methylene blue, dodecylbenzenesulfonic acid (DBSA, commercial grade Bio-Soft S-100, Stepan Chemical, Northfield, IL), and potassium chromate were prepared in deionized water. Butanol, pentanol, hexanol, benzylalcohol, *n*-hexane and chloroform were tested as the immiscible organic phase. Tetraoctylammmonium bromide (TOABr, Sigma-Aldrich) and Amberlite LA-2 (Aldrich), a secondary amine type anion exchanger, were used

without further purification. Typically, solutions were degassed by ultrasonication prior to use.

RESULTS AND DISCUSSION

Stable Stratified Flow. Successful attainment of vertically stratified flows of immiscible liquids was found to be subject to all three factors: device design, intrinsic properties of the liquids and wetted materials and the operating condition (notably flow rate). Regarding the design, the presence of the tongue or interleaf to achieve stable flows before the two fluids contact each other was critical for achieving stable stratified flow, regardless of the other parameters. To some degree it is intuitive that a low interfacial tension (which minimizes the contractile tendency of the interfacial area) must be a key parameter for stable stratification and numerical simulations confirm this. The values of interfacial tension of various organic liquids and water (aqueous solution) and other relevant physical properties are summarized in the Table 1. The interfacial tension between water and short alkyl chain alcohols and benzylalcohol is significantly lower than that between water and other organic solvents. This is presumably due to the presence of the polar hydroxyl groups. In such systems the hydroxyl end of the organic solvent molecule orient themselves towards the aqueous phase at the interface, resulting in a low standard free energy at the interface and hence a low value of interfacial tension[28].

Experiments with the solvents listed in Table I at various flow rates with an optimally designed device showed that at some flow rate stable stratified flows can be achieved for all the alcohols, but not for chloroform or hexane. For these solvents, the layered inlet flow breaks up almost immediately upon entering the channel and results in

an axially segmented or side-by-side flow. Interestingly, addition of ~30 % of butanol into either these organic solvents resulted in sufficient change in the properties that dynamically stable strata could be formed.

The density of the immiscible liquids did not have a significant effect on the stability of the flows. In agreement with the numerical simulations, stable horizontally layered flow of water (colored by a little dye for visualization) and butanol could be achieved with either water on top or butanol on top. Once stable flow was formed, the device could also be turned over without disrupting the stratification.

When we first began experiments with butanol and water, numerical simulations had not been performed. Initial experiments were performed around a flow velocity of 0.5 mm s^{-1} and resulted in segmentation. We presumed that a slower flow would stabilize the interface but segmentation persisted at slower flow; indeed segmentation frequency increased and segment size decreased. When we increased the flow velocity to 1 mm s^{-1}, stable stratification was observed. The transition from segmented to stratified flow thus occurred experimentally between 0.5 and 1 mm s^{-1}, whereas subsequent numerical predictions suggested a transition occurring between 15-20 mm s^{-1}. Admittedly there is a substantial difference between theory and experiment in the exact velocities at which the transition occurs but the model does predict the correct effect of the flow velocity. The three-layer gasket device is considerably more complex than the device modeled. Also, we did not take into account the contact angle with the composite polymer wall, and neglected the significant mutual solubility of the solvents. Regarding the prediction of the model as to the segment length, it can be observed in Figure 1 that near the flow velocities where transition occurs from segmented to stratified flow,

segment length increases with increasing flow velocity until stratified flow is observed. Experimentally, we observe the same trend in segment length as a function of flow velocity just before stratified flow occurs.

It is interesting to note that the observed flow interface is not flat but assumes a curved shape. The surface is driven to minimize the curvature of the interface, which tends in turn to reduce the interfacial area, but it is subject to the condition that the contact angle boundary condition must be satisfied. For any contact angle other than 90°, the result is a curved surface. If the resulting bowed interface contacts the top or bottom of the channel, then the stratified flow structure will be disrupted. Thus we see that the wall contact angle will limit the attainable w/d ratio of the channel for successful attainment of vertically stratified flow.

Further, numerical simulations show that the interface does not remain at the z=0 plane, but within a very short distance (~0.5 mm) from the inlet it has moves down and assumes a finite curvature with the water layer being thinner near the wall than the center of the flow channel. Figure 3 shows the computed device cross-section halfway through the device (y = 22.5 mm). While further plots are not shown, once the interface assumes this shape, it is maintained and does not vary with downstream position. Either the head pressure or flow rates may be adjusted to vary the average height of this interface.

Applications.

Continuous Extraction. The extraction of Methylene Blue (MB) from an aqueous phase to an immiscible organic solvent was studied in the vertically stratified flow device. Aqueous MB solution (1 mM) was aspirated as the bottom layer and an immiscible short

chain aliphatic alcohol was the top liquid in the channel. The upper organic phase with the extracted MB was collected, diluted with the same solvent and its absorbance was measured at 656 nm. The results of varying the flow rates between 20 and 160 μL min^{-1} (per liquid, flow velocity ca. 1 – 8 mm s^{-1}) is shown in Figure 4a. The efficiency of the extraction increases with decreasing the flow rate, as greater residence time in the device is available. The near-linear increase with the residence time suggests that the system is very far from equilibrium for these limited extraction times with this device with d = 380 μm. A significant difference between the amount of MB extracted into the different alcohols is also readily noticeable in Figure 4a. The fact that hexanol displays very poor efficiency in extracting MB can be advantageously used for the determination of an anionic surfactant which uses the ion-pair extraction of the analyte with MB.

Figure 4b shows the effect of the channel depth on the extraction. Butanol was used as a solvent and the three cases differed only in the channel depth. Comparison is made here with the different devices being operated at the same linear velocities, i.e., at the same residence time. The mean diffusion path of the analyte MB increases by factor of ~2.5 from d = 150 μm to 380 μm. As may be expected, the decrease in d clearly favors the efficiency of the extraction. It should be noted that the absolute difference between the channels with different d values increases with decreasing flow velocity. This means that as extraction becomes more complete, the importance of a smaller diffusion distance also increases. Note also that for the shallower devices where extraction efficiency *is* higher, the amount extracted no longer increases linearly with residence time; this too is expected.

If in a similar channel of 2000 μm x 380 μm cross section, we have side by side flow, the mean diffusion distance will increase by more than a factor of 5 and extraction rates will be much lower. In an actual experiment with a device constructed to have parallel inlets and outlets and with individual liquid flow rates at (a) 20 and (b) 160 μL min^{-1}, the observed absorbance of the exit organic liquid was (a) 17 and (b) 100 times lower than the stratified flow case, dramatically demonstrating the advantage of the stratified flow, especially at short contact times.

The separation of phases at the device exit is an issue of practical importance. For most analytical purposes, it is sufficient to get one specific stream containing just one pure phase that is measured; the other can be a mixture of two phases that may be discarded. In the present system, the relative thickness of each fluid layer was adjusted by adjusting the head pressures of the fluid reservoirs. Whichever particular phase we wanted in pure form, we made this to be the thicker layer and the stratified exit located at the halfway point provided that phase in pure form while the other stream was a mixture of two phases and was discarded. With the water-butanol system, we *did* attain 100% separation of water and butanol at the outlet of the device after careful head pressure control. Whether this can be sustained over long periods of time and how robustly this can be maintained has not been studied in detail.

Ion-pair Extraction. Determination of Anionic Surfactants.

As previously noted, the extraction efficiency of MB into hexanol is rather poor but in the presence of an anionic surfactant such as DBSA, an ion-pair is formed that is easily

extracted. This was used to construct a miniature solvent extraction system for measuring anionic surfactants, similar to a standard method that exists for such a determination.[29] A 200 μM aqueous solution of methylene blue (MB) was aspirated through the bottom channel and hexanol was aspirated through the top. The aqueous DBSA sample (0-20 ppm) was introduced into the MB stream by an injection valve upstream of the extraction device. The extracted ion pair of MB^+-$DBSA^-$ was measured with the flow-through detector. The response behavior is depicted in Figure 5a. The response was linear in the range studied ($r^2 = 0.9980$). The repeatability is shown at 12 and 6 ppm DBSA concentrations in Figures 5b and 5c, respectively; The RSD values are 3.3% and 8.6% (n=10). Blank (DI water) injections in the system produce small negative peaks (due to dilution of the dye). Injection of local tap water, however, shows significant positive response.

Sometimes even side-by-side flows can be unstable with respect to segmentation. For this reason, it may be necessary to micromachine guide structures at the bottom of the channels that stabilize the flow.[30] In intrinsically stable layered or side-by-side flow, if the flow rate of a specific liquid is increased, the volume occupied by that liquid in the channel increases accordingly, i.e., in the case of layered flow, it occupies more of the available depth, in the case of side-by-side flow, it occupies more of the available width. If specific guide structures are machined into a device then this ability to control the extent of real estate occupied by a given liquid is lost.

In the present case, this control of relative layer thickness can be readily carried out via control of the hydrostatic head on the liquid reservoirs and the aspiration flow rates. We found it simple to change the aqueous:organic layer thickness from 1:1 (at

which all other data were obtained) to 1:3. In the above DBSA measurement system, as may be intuitive, the highest signals are obtained when the organic: aqueous flow rate ratio is the lowest. Best peak shapes were also achieved under these conditions.

Ion-pair Extraction of Chromate into Butanol. Adding a suitable phase transfer agent to the organic phase allows ion exchange based ion-pair extraction. The chromate ion is not normally extracted into butanol, e.g. no peaks were observed when chromate ion was injected into 10 mM NaOH and the extracting phase was pure butanol (Figure 6). However, the presence of the tetraoctylammonium ion (TOA^+) in the butanol layer, added as 2% TOABr, readily allows the extraction of CrO_4^{2-} into the organic phase. Aqueous 10 mM NaOH was used as a carrier solution and aqueous solution of potassium chromate was injected into this stream. The repeatability of 1 mM K_2CrO_4 injections is shown in Figure 6. The observed RSD was 2.6% (n=12).

Conductivity suppression

In a previous publication[1] we demonstrated continuous ion exchange in a shallow planar channel using side-by-side flows. An organic phase containing a lipophilic ion exchanger flowed next to a simulated ion chromatographic aqueous eluent stream (for cation chromatography) containing 1-10 mM HCl. A strongly basic compound, such as tetraoctylammonium hydroxide (TOAOH), or a secondary amine, e. g., Amberlite LA-2, were used in the organic solvent and proved to be equally efficient for suppression of the conductivity of the eluent phase. The addition of TOAOH to butanol was found to affect the stratified flow in an adverse way (presumably due to changes of the interfacial tension). Amberlite LA-2, which exhibited no such effect, was therefore used

exclusively in this study. Figure 7a shows response to injections of NaCl into a 1 mM HCl carrier, using 1% Amberlite LA-2 in butanol as the ion exchanger. Figure 7b shows repeatability, the observed reproducibility is 0.8 % in RSD (n=10). The response was linear in the range 0-2 mM NaCl (r^2 = 0.9986), the estimated S/N=3 limit of detection (LOD) is $\leq$ 0.1 mM NaCl. This is largely limited by dispersion in the injector and the upstream components as well as the larger than optimum detection cell and dated detector electronics.

Conclusions

We have shown that continuous vertically stratified flow can be achieved in small planar channels and that characteristics, including (in)stability of such flow can be numerically modeled. This theoretical predictability is perceived to be of great utility as a design tool. Compared to side-by-side flows, the vertically layered flow structure is more easily scaled by changing width of a channel, without loss of performance. Layer thicknesses can be readily changed. The applicability of such systems was demonstrated by continuous extraction of methylene blue into different organic solvents, flow-injection (FI) style determination of an anionic surfactant via ion-pair extraction, FI and ion exchange based ion-pair extractive determination of chromate and ion exchange based conductivity suppression.

Table 1. Physical properties of various organic liquids.

	γ_i [a]	γ_0 [a]	ρ [b]	η [b]
Butanol	2.1	24.6	0.81	2.9
Pentanol	4.9	25.4	0.81	4.4
Hexanol	6.8	25.8	0.81	5.1
Benzylalcohol	4.8	39.7	1.04	5.8
Chloroform	32.8	27.1	1.49	0.6
Hexane	51.1	18.4	0.66	0.3

γ_i interfacial tension of respective solvent and water ($mN.m^{-1}$)
γ_0 surface tension against air at 20° C ($mN.m^{-1}$)
ρ density ($g.cm^{-3}$)
η Dynamic viscosity at 20° C
[a] from ref [26]
[b] from ref [30]

FIGURE LEGENDS

Figure 1. Butanol (white) /water (black) and chloroform (white) /water (black) flow simulations at various inlet flow rates. Simulation assumes left/right symmetry; figures show only right half of channel. Full channel dimensions: 0.4 x 2 x 45 mm (*d*-*w*-*l*).

Figure 2. Experimental device, schematically shown. GS1 and GS2: glass slides, schematically shown. G1,T and G2 constitute together a three-layer gasket; on the inlet side, T sticks out into the flow path like a tongue. The assembly is held together by binder clips.

Figure 3. Computed fluid-interface profile midway through the de

Figure 4. The effect of the flow rate (a) and channel depth (b) on the extraction efficiency of methylene blue. Conditions: (a) channel depth: 400 μm, (◆,◇)-butanol, (●,○)-pentanol, (▲,△)-hexanol, (b) flow rate: 40 μL min^{-1}, channel depth : (◆,◇)-150 μm, (●,○)-240 μm, (▲,△)-380 μm. Solid line-extraction efficiency vs. flow rate, broken line- extraction efficiency vs. residence time.

Figure 5. Extraction of DBSA-MB ion pair into hexanol. (a) Response to 4-20 ppm DBSA, (b, c) Repeatability at 12 and 6 ppm DBSA. Conditions: channel depth 380 μm, flow rate 40 μL min^{-1}, injection volume 5 μL, absorbance measured at 565 nm.

Figure 6. Extraction of chromate by ion exchange. (a)Repeatability of 1 mM K_2CrO_4 injections. Conditions: channel depth 380 μm, flow rate 40 μL min^{-1}, injection volume 5 μL, absorbance measured at 372 nm, organic phase = 2% TOABr in

butanol.(b) Blank- 5 injections of 1 mM K_2CrO_4 into 10 mM NaOH, organic phase = butanol without any TOABr. Conditions are same as in (a).

Figure 7. Ion exchange/suppression in stratified flow. (a) Response to NaCl injected into a 1 mM HCl carrier. (b) repeatability, 1 mM NaCl injections. Ion exchanger: 1% Amberlite LA-2 in butanol. Conditions: channel depth 380-μm, flow rate 20 $\mu L.min^{-1}$, injection volume 5 μL, conductivity detection.

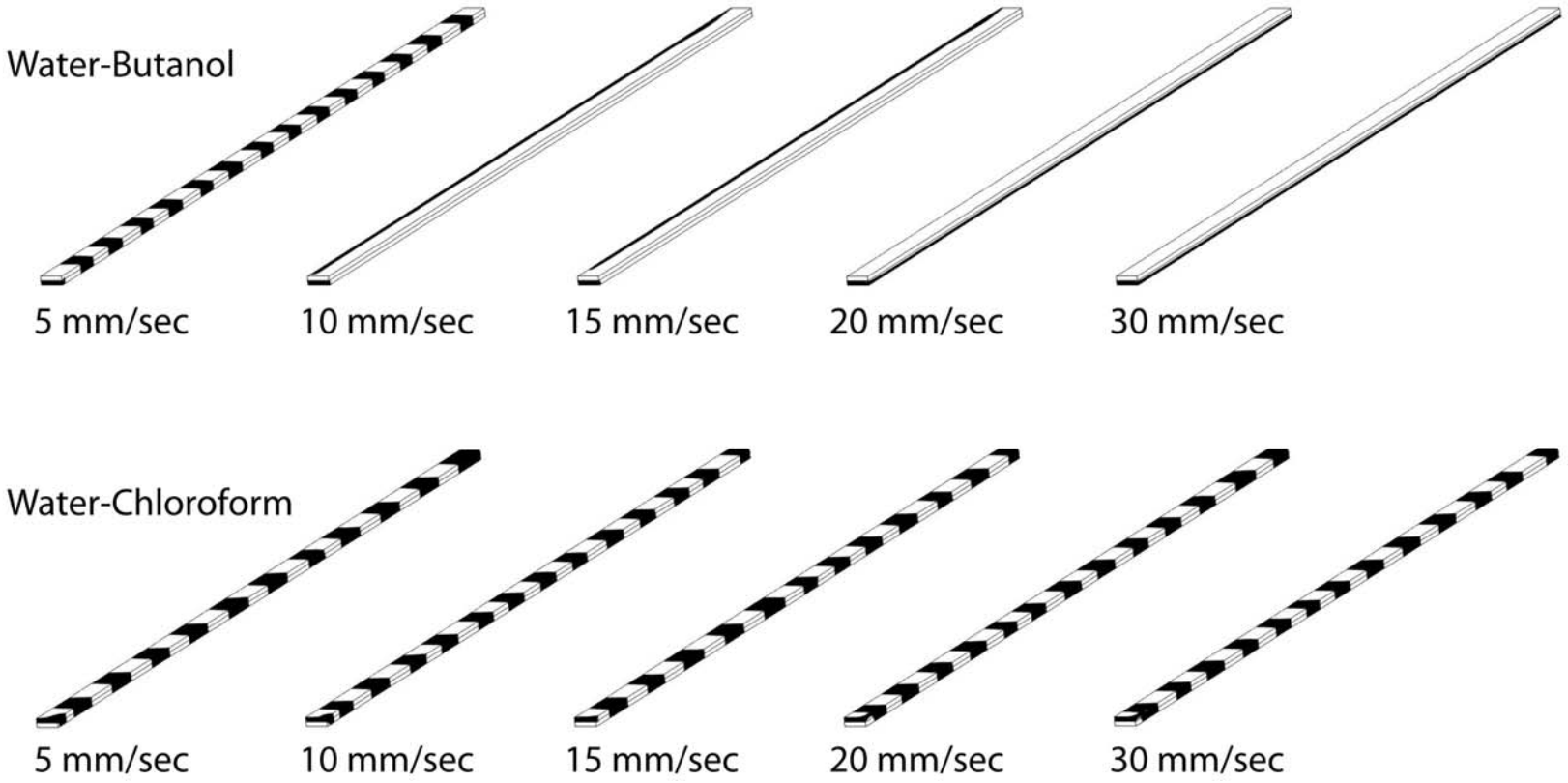
Water-Butanol
5 mm/sec
10 mm/sec
15 mm/sec
20 mm/sec
30 mm/sec
Water-Chloroform
5 mm/sec
10 mm/sec
15 mm/sec
20 mm/sec
30 mm/sec

Figure 1

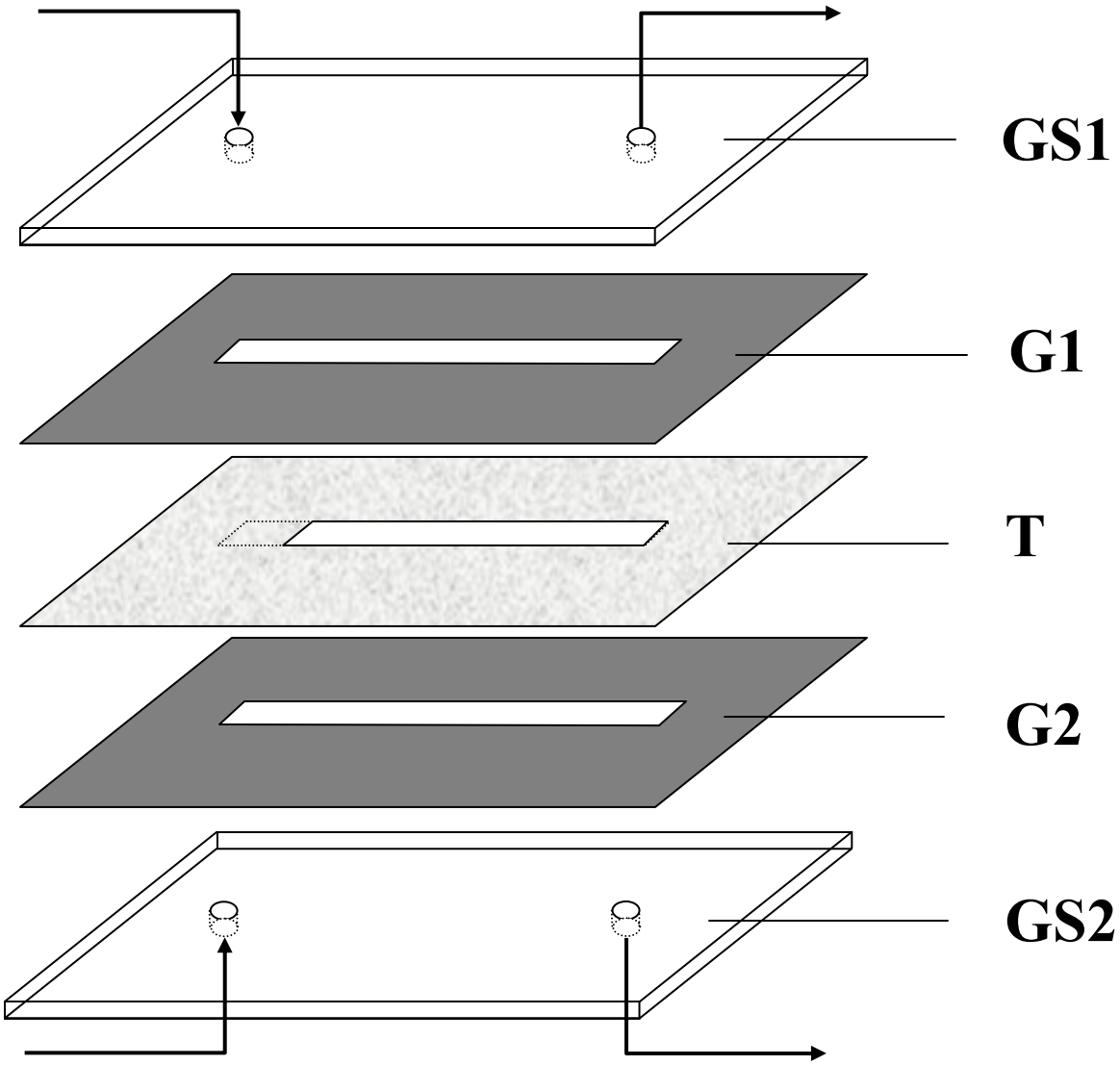

Figure 2.

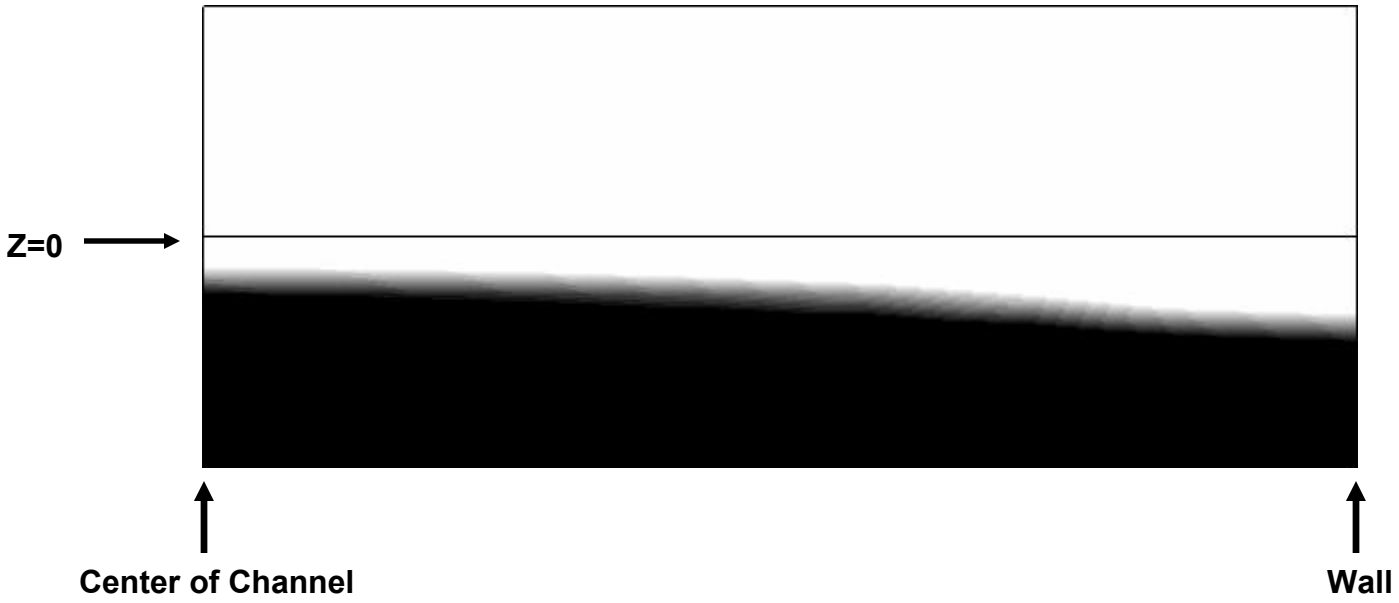

Figure 4

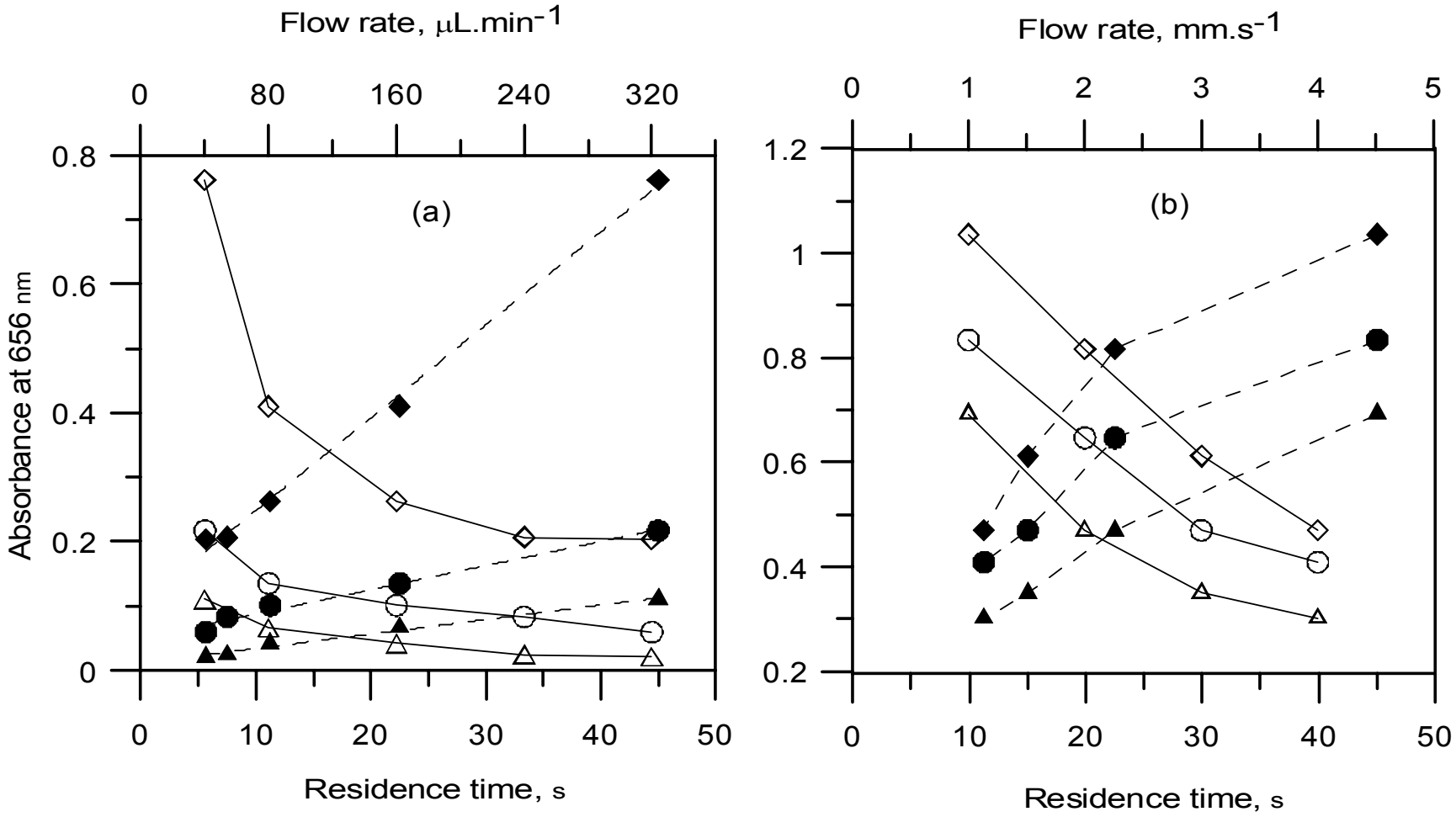
Flow rate, μL.min-1
0
80
160
240
320
(a)
Absorbance at 656 nm
0.8
0.6
0.4
0.2
0
0
10
20
30
40
50
Residence time, s
Flow rate, mm.s-1
0
1
2
3
4
5
(b)
1.2
1
0.8
0.6
0.4
0.2
0
10
20
30
40
50
Residence time, s

Figure 4

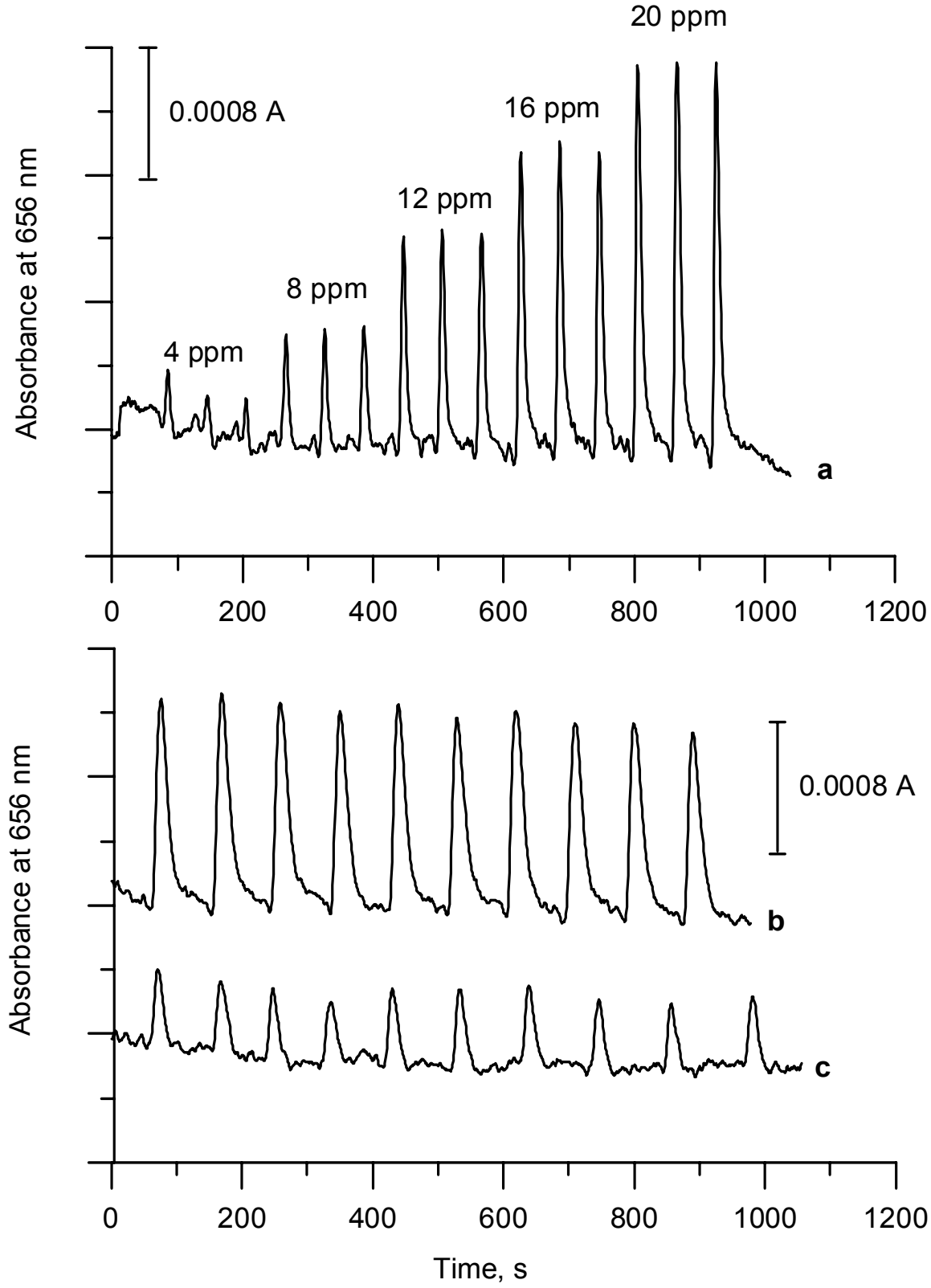
20 ppm
16 ppm
12 ppm
8 ppm
4 ppm
0.0008 A
Absorbance at 656 nm
a
0
200
400
600
800
1000
1200
0.0008 A
b
c
Absorbance at 656 nm
Time, s

Figure 5

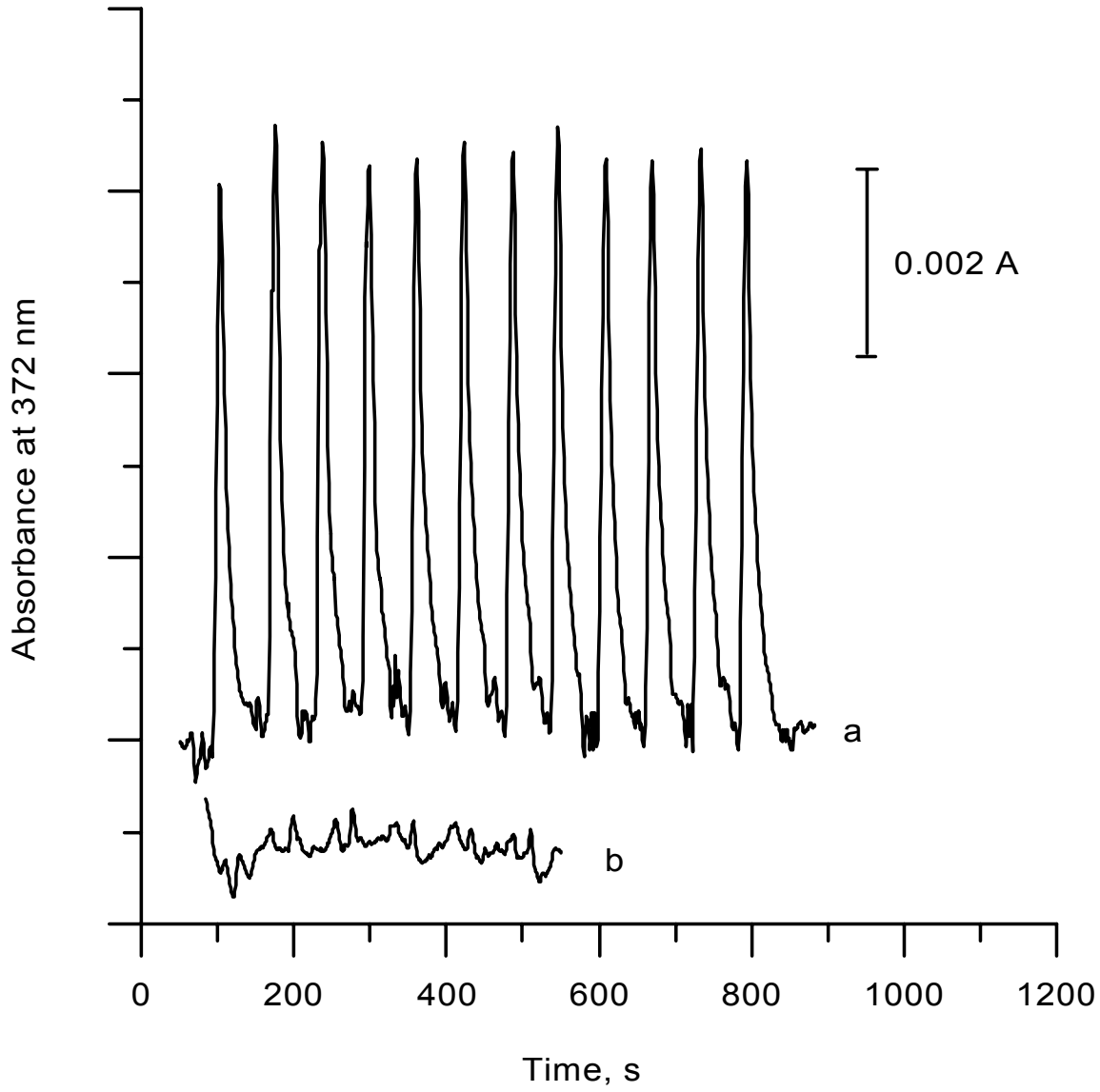
Absorbance at 372 nm
0.002 A
a
b
0
200
400
600
800
1000
1200
Time, s

Figure 6

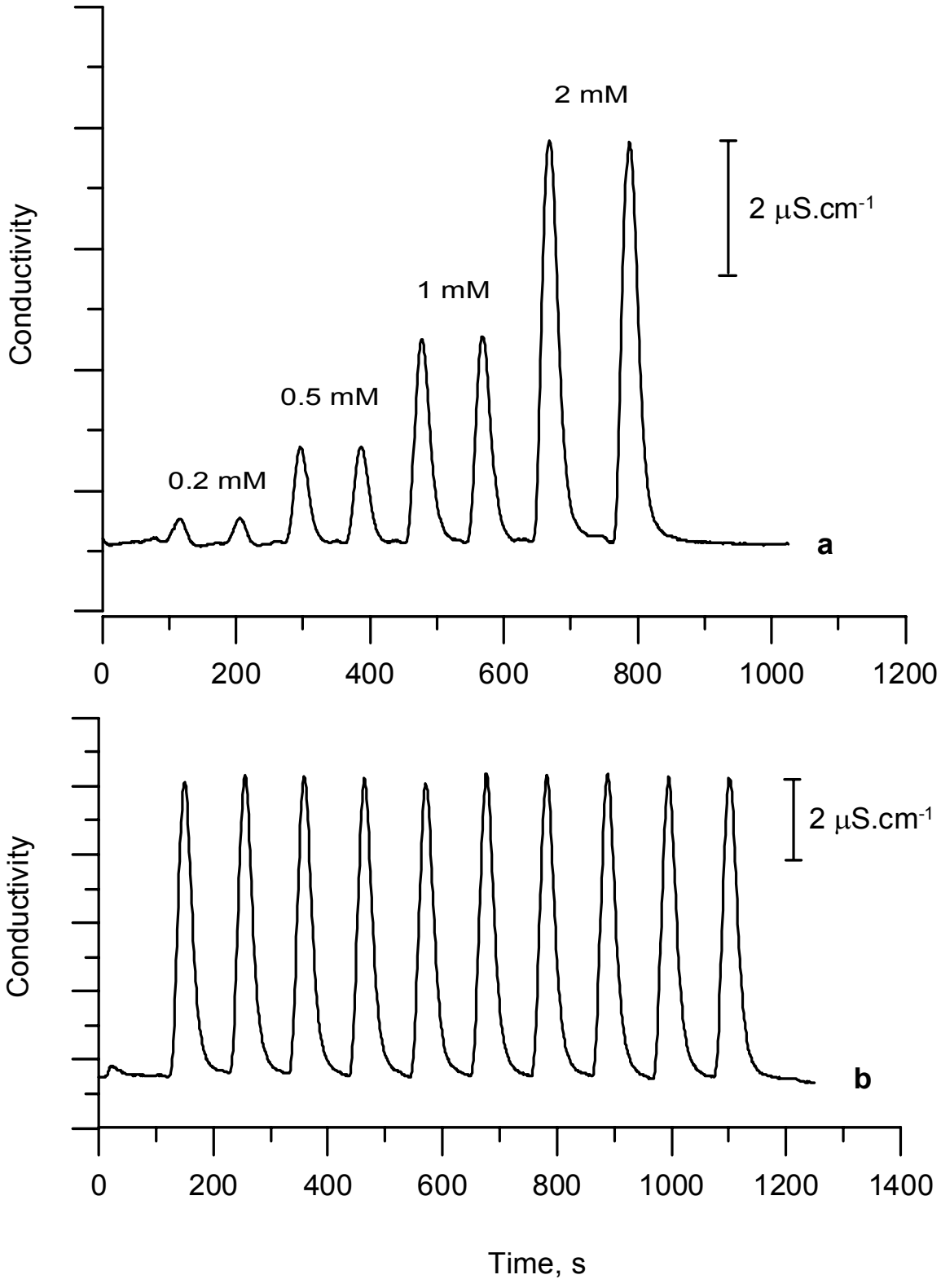
Conductivity
0.2 mM
0.5 mM
1 mM
2 mM
2 μS.cm-1
a
0
200
400
600
800
1000
1200
Conductivity
2 μS.cm-1
b
0
200
400
600
800
1000
1200
1400
Time, s

Figure 7

REFERENCES:

[1] P. Kuban, P. K. Dasgupta and K. A. Morris, *Anal. Chem.* **74,** 5667-5675 (2002).
[1] Yager, P.; Weigl. B. H.; Brody, J. P.; Holl, M. R. US Patent 5,716,852, February, 1998.
[3] Weigl, B.H.; Yager, P. *Science* **1999**, 346-347.
[4] Kamholz, A. E.; E. A. Schilling, Yager, P. *Biophys. J.* **2001,** *80***,** 1967-1972.
[5] Yager, P.; Brody, J. P.; Holl, M. R.; Forster, F. K.; Galambos, P. C. US Patent 5,932,100.
[6] Kamholz, A.E.; Weigl, B.H., Finlayson, B.A.; Yager, P. *Anal. Chem.* **1999**, 71, 5340-5347.
[7] Hatch, A.; Kamholz, A. E.; Hawkins, K. R.; Munson, M. S.; Schilling, E. A.; Weigl, B. H.; Yeager, P. *Nature Biotechnol.* **2001,** *19,* 461-465.
[8] Sato, K.; Tokeshi, M.; Kitamori, T.; Sawada, T. *Anal. Sci.* **1999**, 15, 641-645.
[9] Tokeshi, M.; Minagawa, T.; Kitamori, T. *J. Chromatogr. A*. **2000**, 894, 19-23.
[10] Sato, K. Tokeshi, M.; Sawada, T.; Kitamori, T. *Anal. Sci.* **2000**, 16, 455-456.
[11] Surmeian, M.; Hibara, A.; Slyadnev, M.; Uchiyama, K.; Hisamoto, H.; Kitamori, T. *Anal. Lett.* **2001**, 34, 1421-1429.
[12] Tokeshi, M.; Minagawa, T.; Kitamori, T., *Anal. Chem.* **2000**, *72*, 1711-1714
[13] Hisamoto, H.; Horiuchi, T.; Tokeshi, M.; Hibara, A.; Kitamori, T. *Anal. Chem.* **2001**, 73, 1382-1386.
[14] Hibara, A.; Tokeshi, M.; Uchiyama, K.; Hisamoto, H.; Kitamori, T. *Anal. Sci.* **2001**, *17*, 89-93.
[15] http://www.micronics.net/technologies/h_filter.php; http://www.micronics.net/technologies/t_sensor.php
[16] Shaw, J.; Nudd, R.; Naik, B.; Turner, C.; Rudge, D.; Benson, M.; Garman, A. *Proceedings of Micro Total Analysis Systems 2000*; van den Berg, A., Olthuis, W., Bergveld, P., Eds., Kluwer Academic Publishers: Dordrecht, The Netherlands, 2000; pp 371-374; Ehrfeld, W.; Hessel, V.; Löwe, H. *Microreactors*; Wiley-VHC: Weiheim, 2000; Chapter 5.
[17] Zhao, B.; Moore, J. S.; Beebe, D. J. *Science* **2001**, *291*, 1023-1026; *Anal. Chem.* **2002,** *74,* 4259-4268.
[18] Zhao, B., Viernes, N. O., Moore, J. S., Beebe, D. J., J. Am. Chem. Soc., **2002**, *124*, 5284-5285
[19] Hibara, A.; Nonaka, M.; Hisamoto, H.; Uchiyama, K.; Kikutani, Y.; Tokeshi, M.; Kitamori, T. *Anal. Chem.* **2002,** *74,* 1724-1728.
[20] http://ourworld.compuserve.com/homepages/anima/khi.htm
[21] http://flash.uchicago.edu/~zingale/rt_gallery/rt_gallery.html
[22] Drazin, P. G., *Introduction to Hydrodynamic Stability*, Cambridge University Press, Cambridge, UK, 2002
[23] Collier, J. G.; Thome, J. R. *Convective boiling and condensation*, Oxford University, 3rd ed., 1996.
[24] CFD Research Corporation, *CFD-ACE(U) Module Manual Version 2002*, CFDRC, Huntsville, AL, June 2002.
[25] Hirt, C.W.; Nichols, B.D. *J. Comput. Phys.* **1981,** 39, 201–225.
[26] John, F., *Partial Differential Equations*, Springer-Verlag, NY, 1986, pp. 6–8.
[27] National Research Council, International Critical Tables, 1930. NRC, Washington D.C.
[28] J.T. Davies, E.K. Rideal, Interfacial Phenomena, Academic Press, NY, USA, 1961.
[29] Clessceri, L. S.; Greenberg, A. E.; Trussell, R. R. *Standard Methods for the Examination of Water and Wastewater*, 17th ed., 1989. American Public Health Association, Washington D. C. Method 5540C. Anionic Surfactants as MBAS. 5-59-5-63.
[30] Surmeian, M.; Slyadnev, M. N.; Uchiyama, K.; Hisamoto, H.; Hibara, A.; Uchiyama, K.; Kitamori, T. *Anal. Chem.* **2002**, 74, 2014-2020.
[30] CRC Handbook of Chemistry and Physics, 55th Edition, CRC Press, 1974.